Frontiers in Applied Mathematics and Statistics

TYPE Original Research
PUBLISHED 03 November 2022
DOI 10.3389/fams.2022.963991

Prey fear of a specialist predator in a tri-trophic food web can eliminate the superpredator

Nabaa Hassain Fakhry[1], Raid Kamel Naji[1], Stacey R. Smith?[2] and Mainul Haque[3]*

[1]Department of Mathematics, College of Science, University of Baghdad, Baghdad, Iraq, [2]Department of Mathematics and Faculty of Medicine, The University of Ottawa, Ottawa, ON, Canada, [3]School of Mathematical Science, The University of Nottingham Ningbo China, Ningbo, China

OPEN ACCESS

EDITED BY
Aurelio A. de los Reyes V,
University of the Philippines
Diliman, Philippines

REVIEWED BY
Pankaj Tiwari,
University of Kalyani, India
Abdelalim A. Elsadany,
Suez Canal University, Egypt

*CORRESPONDENCE
Mainul Haque
Mainul.Haque@nottingham.edu.cn

SPECIALTY SECTION
This article was submitted to Mathematical Biology, a section of the journal Frontiers in Applied Mathematics and Statistics

RECEIVED 08 June 2022
ACCEPTED 05 October 2022
PUBLISHED 03 November 2022

CITATION
Fakhry NH, Naji RK, Smith? SR and Haque M (2022) Prey fear of a specialist predator in a tri-trophic food web can eliminate the superpredator. *Front. Appl. Math. Stat.* 8:963991. doi: 10.3389/fams.2022.963991

We propose an intraguild predation ecological system consisting of a tri-trophic food web with a fear response for the basal prey and a Lotka–Volterra functional response for predation by both a specialist predator (intraguild prey) and a generalist predator (intraguild predator), which we call the superpredator. We prove the positivity, existence, uniqueness, and boundedness of solutions, determine all equilibrium points, prove global stability, determine local bifurcations, and illustrate our results with numerical simulations. An unexpected outcome of the prey's fear of its specialist predator is the potential eradication of the superpredator.

KEYWORDS

intraguild predation, food web, fear effect, stability, specialist predator

Introduction

A functioning ecosystem depends on the framework of food webs that it supports [1]. Food webs involve many types of predator–prey interactions, which are fundamental interactions for sustaining species [2]. Interaction between the prey and the predator can be affected by factors such as refuge, disease, stage structure, competition, and fear [3–7]. Intraguild predation (IGP), on the other hand, is described as predator–prey interactions among consumers who may be fighting for limited resources. In natural communities, there is a growing body of literature emphasizing the relevance of intraguild predation [8, 9]. Three species are involved in the simplest intraguild predation model: a superpredator (IG predator), a specialist predator (IG prey), and a basal prey. Bai et al. recently suggested a three-species IGP food web model with the IG predator, IG prey, and basal prey, in which the basal prey grows logistically with a large Allee effect [10]. They looked into the model's local and global dynamics, focusing on the impact of the Allee effect and discovered that the intraguild predation food web model has rich and complicated dynamic behavior and that a large Allee effect in the basal prey raises the danger of extinction for not only the basal prey but also the IG prey or/and IG predator.

Many predators in food webs are superpredators, who may not restrict their diets to a specific prey species but feed also on other predators [11]. Therefore, superpredators are expected to compete not only with other predators for food and space but in many cases also through intraguild predation [5, 12, 13]. Predators induce indirect effects such as fear in prey that can change the prey's behavior [14]. Fear takes the form of sustained psychological stress on the prey, as prey species are always wary of possible attack [15]. Suraci et al. experimentally showed that fear of large carnivores reduces mesocarnivore foraging, which benefits the mesocarnivore's prey [16].

A handful of mathematical models have studied the effect of fear on food webs. Panday et al. investigated the impact of fear in a tri-trophic food chain model, with prey fear in response to both predators [15], from the middle predator to the generalist predator [17] and with delays [18]. Cong et al. introduced a fear-adjusted birth rate to a three-species food web [19]. Hossain et al. limited the growth of the prey due to fear in an intraguild predation model [20]. Mukerjee incorporated interspecific competition and fear affecting the death rate of the prey [21]. Ibrahim et al. limited prey growth due to fear of the generalist predator and showed that fear could have a stabilizing effect on the system [22]. Mondal et al. showed that the prey's fear of predators was responsible for the increase in intraspecific competition among the prey species [23]. Roy et al. showed that fear could play a destablizing role if it caused a reduction in the birth rate of susceptible prey, whereas the levels of fear responsible for the increase in the intraspecies competition of susceptible prey and eradication of the disease prevalence could stabilize an otherwise unstable system [24]. Maity et al. considered time-varying fear effects, showing that periodic solutions could arise [25]. Hossain et al. showed that perceived fear of predators could reduce the prey birth rate [26]. Tiwari et al. showed that seasonal variations in the level of prey fear generated higher-order periodic solutions [27].

Here, we examine the impact of fear on the dynamical behavior of an IGP food web system in which the prey responds with fear to the specialist predator but not the superpredator; because the superpredator has alternative food sources, it will be less dangerous to the basal prey compared to the IG prey. To the best of our knowledge, this is the first model to examine this effect.

Food-web model formulation

Our food web consists of a prey at the first level, a specialist predator at the second level, and a superpredator at the third level. Let $x(t)$, $y(t)$, and $z(t)$ be the population densities at time t for the prey, specialist predator, and superpredator, respectively. The prey grows logistically in the absence of predators, while it has a fear property of predation in the presence of the specialist predator. Hence, the intrinsic growth rate of prey becomes $\frac{r}{1+ky}$, which is a monotonic decreasing function of both k and y, where k represents the fear rate [28]. The food transport attack rates are given by the parameters a_1, a_2, and a_3, with conversion rates e_1, e_2, and e_3. Finally, the predators face natural death rates d_1 and d_2 for the specialist predator and superpredator, respectively. The dynamics of the food web with fear can be represented mathematically by the following set of differential equations:

$$\begin{aligned}
\frac{dx}{dt} &= rx(1-x)\left(\frac{1}{1+ky}\right) - a_1xy - a_2xz = xf_1(x,y,z),\\
\frac{dy}{dt} &= e_1a_1xy - a_3yz - d_1y = yf_2(x,y,z),\\
\frac{dz}{dt} &= e_2a_2xz + e_3a_3yz - d_2z = zf_3(x,y,z).
\end{aligned} \tag{1}$$

Initial conditions satisfy $x(t) \geq 0, y(t) \geq 0$, and $z(t) \geq 0$, and all parameters are assumed to be positive.

The interaction functions f_i $(i = 1, 2, 3)$ are continuous and have continuous partial derivatives and are thus Lipschitzian, so system (1) has a unique solution. Furthermore, for any initial condition in $\mathbb{R}^3_+$, the solution of system (1) is positive and uniformly bounded as shown in the following theorem. Hence, system (1) will be a dissipative system.

Theorem (1): The domain of system (1), $\mathbb{R}^3_+$, is positively invariant, and all solutions of system (1) starting in $\mathbb{R}^3_+$ are uniformly bounded.

Proof. Let $x(t), y(t)$, and $z(t)$ be any solution of system (1). Since the solution $(x(t), y(t), z(t))$ of the system (1) with initial condition in $\mathbb{R}^3_+$ exists and is unique on $[0\ ,\ \delta)$, where $0 < \delta \leq +\infty$, we have:

$$x(t) = x(0)\, e^{\int_0^t \left[r(1-x(s))\left(\frac{1}{1+ky(s)}\right)-a_1y(s)-a_2z(s)\right]ds} \geq 0$$

$$y(t) = y(0)\, e^{\int_0^t \left[e_1a_1x(s)-a_3z(s)-d_1\right]ds} \geq 0$$

$$z(t) = z(0)\, e^{\int_0^t \left[e_2a_2x(s)+e_3a_3y(s)-d_2\right]ds} \geq 0.$$

From the first equation of system (1):

$$\frac{dx}{dt} \leq rx(1-x).$$

Then, it is easy to verify that $x(t) \leq \frac{r}{4}$ for all t.

Let $= x + y + z$. Then, since $e_i \in (0, 1)$; $i = 1, 2, 3$, we have $\frac{dW}{dt} \leq \frac{r}{4} - M\left[x + y + z\right]$,
where $M = \min\left\{1, d_1, d_2\right\}$. Solving the following linear differential inequality

$$\frac{dW}{dt} + MW \leq \frac{r}{4},$$

we obtain that, as $t \to \infty$,

$$W(t) \leq \frac{r}{4M}.$$

Existence of equilibrium points

System (1) has at most five nonnegative biologically feasible equilibrium points. The trivial equilibrium $E_0 = (0, 0, 0)$ always exists. The axial equilibrium $E_1 = (1,0,0)$ always exists on the boundary of the first octant. The specialist-free equilibrium point, $E_2 = (\bar{x}, 0, \bar{z})$, where

$$\bar{x} = \frac{d_2}{e_2 a_2} \text{ and } \bar{z} = \frac{r(1-\bar{x})}{a_2}, \tag{2a}$$

exists provided that

$$d_2 < e_2 a_2. \tag{2b}$$

The superpredator-free equilibrium point, $E_3 = \left(\hat{x}, \hat{y}, 0\right)$, where

$$\hat{x} = \frac{d_1}{e_1 a_1} \text{ and } \hat{y} = -\frac{1}{2k} + \frac{1}{2a_1 k}\sqrt{a_1^2 + 4kr\frac{\left(e_1 a_1 - d_1\right)}{e_1}}, \tag{3a}$$

exists, provided that

$$d_1 < e_1 a_1. \tag{3b}$$

There is also an interior equilibrium point, $E_4 = \left(x^*, y^*, z^*\right)$, where

$$y^* = \frac{d_2 - e_2 a_2 x^*}{e_3 a_3} \text{ and } z^* = \frac{e_1 a_1 x^* - d_1}{a_3}, \tag{4a}$$

with x^* a positive root of the following second-order polynomial equation:

$$\beta_1 x^2 + \beta_2 x + \beta_3 = 0, \tag{4b}$$

where

$$\beta_1 = e_2 a_1 {a_2}^2 k \left[e_1 e_3 - e_2\right],$$

$$\begin{aligned}\beta_2 = e_2 e_3 a_1 a_2 a_3 - r{e_3}^2{a_3}^2 + 2e_2 a_1 a_2 k d_2 - e_1 e_3 a_1 a_2 {a_3}^2 \\ -e_1 e_3 a_1 a_2 k d_2 - e_2 e_3 {a_2}^2 k d_1,\end{aligned}$$

$$\beta_3 = r{e_3}^2{a_3}^2 - e_3 a_1 a_3 d_2 - a_1 k {d_2}^2 + e_3 a_2 {a_3}^2 d_1 + e_3 a_2 k d_1 d_2.$$

Therefore, there is a unique interior equilibrium point in the interior of $\mathbb{R}^3_+$ provided that the following conditions hold:

$$\frac{d_1}{e_1 a_1} < x^* < \frac{d_2}{e_2 a_2} \tag{4c}$$

$$\left.\begin{matrix}\beta_1 > 0;\ \beta_3 < 0 \\ OR \\ \beta_1 < 0;\ \beta_3 > 0\end{matrix}\right\}. \tag{4d}$$

Persistence

Next, we determine the requirements that ensure persistence in the system (1). Because the types of attractors available in the boundary planes affect the creation of our IGP food web model's persistence conditions, an analysis of the dynamics in the boundary planes of the IGP food web system is conducted. System (1) has two subsystems: the first occurs in the absence of the superpredator (IG predator) and the second occurs in the absence of the specialist predator (IG prey). The first subsystem is

$$\begin{aligned}\frac{dx}{dt} &= x\left[\frac{r(1-x)}{1+ky} - a_1 y\right] = x f_1\left(x,y\right) \\ \frac{dy}{dt} &= y\left[e_1 a_1 x - d_1\right] = y g_1\left(x,y\right).\end{aligned} \tag{5}$$

The second subsystem can be written as follows:

$$\begin{aligned}\frac{dx}{dt} &= x\left[r\left(1-x\right) - a_2 z\right] = x f_2\left(x,z\right) \\ \frac{dz}{dt} &= z\left[e_2 a_2 x - d_2\right] = z g_2\left(x,z\right).\end{aligned} \tag{6}$$

Subsystem (5) has a unique positive equilibrium point in the interior of xy-plane given by $\left(\hat{x}, \hat{y}\right) \equiv E_3$, while subsystem (6) has a unique positive equilibrium point in the interior of xz-plane given by $\left(\bar{x}, \bar{z}\right) \equiv E_2$. The interior equilibrium point of subsystem (5) corresponds to system (1)'s superpredator-free equilibrium point; similarly, the interior equilibrium point of subsystem (6) corresponds to system (1)'s specialist-predator-free equilibrium point. The dynamics around these equilibrium points can be described in the following theorem.

Theorem (2): There are no periodic dynamics in the interior of xy-plane or the xz-plane.

Proof. Define a continuously differential function $B\left(x,y\right) = \frac{1}{xy}$. Then, we have:

$$\Delta = \frac{\partial\left(Bf_1\right)}{\partial x} + \frac{\partial\left(Bg_1\right)}{\partial y} = -\frac{r}{y\left(1+ky\right)}.$$

Clearly, Δ has the same sign and does not equal zero almost everywhere in a simply connected region of the xy-plane. By the Dulac–Bendixson criterion, system (1) has no periodic solutions lying entirely in the interior of $xy-$plane. The second part follows by using the Dulac function $C\left(x,z\right) = \frac{1}{xz}$.

Theorem (3): System (1) is uniformly persistent in the interior of $\mathbb{R}^3_+$, provided that

$$e_1 a_1 > d_1, \tag{7a}$$

$$e_2 a_2 > d_2, \tag{7b}$$

$$e_1 a_1 \bar{x} > a_3 \bar{z} + d_1, \tag{7c}$$

$$e_2 a_2 \hat{x} + e_3 a_3 \hat{y} > d_2. \tag{7d}$$

Proof. Consider the function $\left(x,y,z\right) = x^{b_1}y^{b_2}z^{b_3}$, where $b_i, i = 1,2,3$, are positive constants and $U\left(x,y,z\right)$ is a C^1 nonnegative function in the interior of $\mathbb{R}^3_+$. Hence, we have

$$\frac{dU}{dt} = \frac{\partial U}{\partial x}\frac{dx}{dt} + \frac{\partial U}{\partial y}\frac{dy}{dt} + \frac{\partial U}{\partial z}\frac{dz}{dt},$$

with

$$\frac{\partial U}{\partial x} = b_1 x^{(b_1-1)} y^{b_2} z^{b_3},$$

$$\frac{\partial U}{\partial y} = b_2 x^{b_1} y^{(b_2-1)} z^{b_3},$$

$$\frac{\partial U}{\partial z} = b_3 x^{b_1} y^{b_2} z^{(b_3-1)}.$$

Therefore,

$$\begin{aligned}\Psi\left(x,y,z\right) &= \frac{\left(\frac{dU}{dt}\right)}{U(x,y,z)} = \frac{b_1}{x}\frac{dx}{dt} + \frac{b_2}{y}\frac{dy}{dt} + \frac{b_3}{z}\frac{dz}{dt},\\ &= b_1\left[r\left(1-x\right)\left(\frac{1}{1+ky}\right) - a_1y - a_2z\right]\\ &+ b_2\left[e_1a_1x - a_3z - d_1\right] + b_3\left[e_2a_2x + e_3a_3y - d_2\right].\end{aligned}$$

Since there are no periodic solutions in the boundary planes of the system (1), it follows that system (1) is uniformly persistent provided that $\Psi\left(E_i\right) > 0$ for each $i = 1,2,3$. We have

$$\Psi\left(E_1\right) = b_2\left[e_1a_1 - d_1\right] + b_3\left[e_2a_2 - d_2\right],$$

$$\Psi\left(E_2\right) = b_2\left[e_1a_1\bar{x} - a_3\bar{z} - d_1\right],$$

$$\Psi\left(E_3\right) = b_3\left[e_2a_2\hat{x} + e_3a_3\hat{y} - d_2\right].$$

Consequently, conditions (7a)–(7d) satisfy $\Psi\left(E_i\right) > 0$ for each $i = 1,2,3$.

Global stability analysis

Here, we use Lyapunov functions to investigate the global stability of equilibria.

Theorem (4): The axial equilibrium point $E_1 = (1,0,0)$ is globally asymptotically stable provided that the following sufficient condition holds:

$$e_2 < e_1e_3 < \frac{d_2}{a_2}. \tag{8}$$

Proof. Consider the following positive-definite, real-valued function around E_1:

$$V_1 = c_1\left[x - 1 - \ln x\right] + c_2y + c_3z.$$

Then, we have:

$$\begin{aligned}\frac{dV_1}{dt} &= -\frac{c_1r}{1+ky}\left(x-1\right)^2 - \left(c_1 - c_2e_1\right)a_1xy - \left(c_1 - c_3e_2\right)a_2xz\\ &- \left(c_2 - c_3e_3\right)a_3yz - \left(c_2d_1 - c_1a_1\right)y - \left(c_3d_2 - c_1a_2\right)z.\end{aligned}$$

Then, by choosing $c_1 = e_1$, $c_2 = 1$ and $c_3 = \frac{1}{e_3}$, we obtain

$$\begin{aligned}\frac{dV_1}{dt} &= -\frac{e_1r}{1+ky}\left(x-1\right)^2 - \left(e_1 - \frac{e_2}{e_3}\right)a_2xz - \left(d_1 - e_1a_1\right)y\\ &- \left(\frac{d_2}{e_3} - e_1a_2\right)z.\end{aligned}$$

Clearly, under condition (8), $\frac{dV_1}{dt}$ is negative definite. Moreover, since V_1 is radially unbounded, the axial equilibrium point $E_1 = (1,0,0)$ is globally asymptotically stable.

Theorem (5): The specialist-free equilibrium point $E_2 = (\bar{x},0,\bar{z})$ is globally asymptotically stable provided that the following sufficient conditions hold:

$$a_1\bar{x} < \frac{d_1}{e_1} + \frac{e_3a_3}{e_2}\bar{z}, \tag{9a}$$

$$e_1e_3 < e_2. \tag{9b}$$

Proof. Consider the following positive-definite, real-valued function around E_2:

$$V_2 = c_1\left[x - \bar{x} - \bar{x}\ln\frac{x}{\bar{x}}\right] + c_2y + c_3\left[z - \bar{z} - \bar{z}\ln\frac{z}{\bar{z}}\right].$$

Then, we have:

$$\begin{aligned}\frac{dV_2}{dt} &= -c_1r\left(x-\bar{x}\right)^2 - a_2\left[c_1 - c_3e_2\right]\left(x-\bar{x}\right)\left(z-\bar{z}\right)\\ &- \left(c_1 - c_2e_1\right)a_1xy\\ &- \left(c_2d_1 - c_1a_1\bar{x} + c_3e_3a_3\bar{z}\right)y - \left(c_2 - c_3e_3\right)a_3yz.\end{aligned}$$

Then, by choosing $c_1 = 1$, $c_2 = \frac{1}{e_1}$ and $c_3 = \frac{1}{e_2}$, we have:

$$\begin{aligned}\frac{dV_2}{dt} &= -r\left(x-\bar{x}\right)^2 - \left(\frac{d_1}{e_1} + \frac{e_3a_3}{e_2}\bar{z} - a_1\bar{x}\right)y\\ &- \left(\frac{1}{e_1} - \frac{e_3}{e_2}\right)a_3yz.\end{aligned}$$

Obviously, under conditions (9a)–(9b), $\frac{dV_2}{dt}$ is negative definite. Moreover, since V_2 is radially unbounded, the specialist-free equilibrium point $E_2 = (\bar{x},0,\bar{z})$ is globally asymptotically stable.

Theorem (6): The superpredator-free equilibrium point $E_3 = \left(\hat{x},\hat{y},0\right)$is globally asymptotically stable, provided that, in addition to condition (9b), the following sufficient conditions hold:

$$a_2\hat{x} + \frac{a_3}{e_1}\hat{y} < \frac{d_2}{e_2}, \tag{10a}$$

$$\left(x-\hat{x}\right)\left(y-\hat{y}\right) > 0. \tag{10b}$$

Proof. Consider the following positive-definite, real-valued function around E_3:

$$V_3 = c_1\left[x - \hat{x} - \hat{x}\ln\frac{x}{\hat{x}}\right] + c_2\left[y - \hat{y} - \hat{y}\ln\frac{y}{\hat{y}}\right] + c_3z.$$

Then, we have

$$\frac{dV_3}{dt} = -\frac{c_1 r(x-\hat{x})^2}{R} - \frac{c_1 rk(1-\hat{x})(x-\hat{x})(y-\hat{y})}{R\hat{R}} \\ - (c_1 - c_2 e_1)\, a_1 \left(x - \hat{x}\right)\left(y - \hat{y}\right) - (c_1 - c_3 e_2)\, a_2 xz \\ - (c_2 - c_3 e_3)\, a_3 yz - \left(c_3 d_2 - c_1 a_2 \hat{x} - c_2 a_3 \hat{y}\right) z,$$

where $R = \left(1 + ky\right)$ and $\hat{R} = \left(1 + k\hat{y}\right)$. Then, by choosing $c_1 = 1, c_2 = \frac{1}{e_1}$ and $c_3 = \frac{1}{e_2}$, we obtain:

$$\frac{dV_3}{dt} \leq -\frac{r\left(x - \hat{x}\right)^2}{R} - \frac{rk\left(1 - \hat{x}\right)\left(x - \hat{x}\right)\left(y - \hat{y}\right)}{R\hat{R}} \\ - \left(\frac{1}{e_1} - \frac{e_3}{e_2}\right) a_3 yz - \left(\frac{d_2}{e_2} - a_2 \hat{x} - \frac{a_3}{e_1}\hat{y}\right) z.$$

Under conditions (10a)–(10b), $\frac{dV_3}{dt}$ is negative definite. Since V_3 is radially unbounded, the superpredator-free equilibrium point $E_3 = \left(\hat{x}, \hat{y}, 0\right)$ is globally asymptotically stable.

Theorem (7): The coexistence equilibrium point $E_4 = \left(x^*, y^*, z^*\right)$ is globally asymptotically stable provided that, in addition to condition (9b), the following sufficient condition holds:

$$\left(x - x^*\right)\left(y - y^*\right) > 0. \tag{11}$$

Proof. Consider the following positive-definite, real-valued function around E_4:

$$V_4 = c_1\left[x - x^* - x^* \ln\frac{x}{x^*}\right] + c_2\left[y - y^* - y^* \ln\frac{y}{y^*}\right] \\ + c_3\left[z - z^* - z^* \ln\frac{z}{z^*}\right].$$

Then, we have:

$$\frac{dV_4}{dt} = -\frac{c_1 r\left(x-x^*\right)^2}{R} - \frac{c_1 rk\left(1-x^*\right)\left(x-x^*\right)\left(y-y^*\right)}{RR^*} \\ - (c_1 - c_2 e_1)\, a_1 \left(x - x^*\right)\left(y - y^*\right) \\ - (c_2 - c_3 e_3)\, a_3 \left(y - y^*\right)\left(z - z^*\right) \\ - (c_1 - c_3 e_2)\, a_2 \left(x - x^*\right)\left(z - z^*\right),$$

where $R^* = 1 + ky^*$. Then, by choosing $c_1 = e_2$, $c_2 = e_3$, and $c_3 = 1$, we have

$$\frac{dV_4}{dt} = -\frac{e_2 r\left(x - x^*\right)^2}{R} - \frac{e_2 rk\left(1 - x^*\right)\left(x - x^*\right)\left(y - y^*\right)}{RR^*} \\ - (e_2 - e_1 e_3)\, a_1 \left(x - x^*\right)\left(y - y^*\right).$$

Then, under condition (11) with (9b), $\frac{dV_4}{dt}$ is negative definite. Since V_4 is radially unbounded, the coexistence equilibrium point $E_4\left(x^*, y^*, z^*\right)$ is globally asymptotically stable.

Bifurcation analysis

In this section, we investigate the effect of varying parameter values on the dynamics of the system (1) using local bifurcation analysis and the Sotomayor theorem [29]. First, we rewrite system (1) in the vector form as follows:

$$\frac{dX}{dt} = F\left(X\right), X = \left(x, y, z\right)^T \text{ and } F = \left(xf_1, yf_2, zf_3\right)^T.$$

The second derivative of F with respect to X can be written as:

$$D^2F\left(U, U\right) = \\ \begin{pmatrix} -\frac{2ru_1{}^2}{1+ky} - \frac{2kr(1-2x)u_1u_2}{(1+ky)^2} - 2a_1u_1u_2 - 2a_2u_1u_3 + \frac{2k^2rx(1-x)u_2{}^2}{(1+ky)^3} \\ 2e_1a_1u_1u_2 - 2a_3u_2u_3 \\ 2e_2a_2u_1u_3 + 2e_3a_3u_2u_3 \end{pmatrix}, \tag{12}$$

where $U = (u_1, u_2, u_3)^T$ is a general vector.

Theorem (8): Assume that $d_2 = e_2a_2 \left(\equiv d_2{}^*\right)$. Then system (1) undergoes a transcritical bifurcation at the axial equilibrium point E_1, but neither a saddle node nor a pitchfork bifurcation can occur if

$$e_1a_1 < d_1. \tag{13}$$

Proof. The Jacobian matrix of system (1) at the axial equilibrium point E_1 with $d_2 = e_2a_2 \left(\equiv d_2{}^*\right)$ can be written as:

$$J_1 = J\left(E_1, d_2{}^*\right) = \begin{bmatrix} -r & -a_1 & -a_2 \\ 0 & e_1a_1 - d_1 & 0 \\ 0 & 0 & 0 \end{bmatrix}.$$

J_1 has eigenvalues $\lambda_{11}{}^* = -r < 0$, $\lambda_{12}{}^* = e_1a_1 - d_1 < 0$ under condition (13), and $\lambda_{13}{}^* = 0$. Hence, the necessary but not sufficient condition for a bifurcation is satisfied, and E_1 is a non-hyperbolic point.

Let $\Phi_1 = (v_{11}, v_{12}, v_{13})^T$ be the eigenvector of J_1 corresponding to the eigenvalue $\lambda_{13}{}^* = 0$. Straightforward computation gives $\Phi_1 = (\beta_1 v_{13}, 0, v_{13})^T$, where v_{13} represents any nonzero real number and $\beta_1 = -\frac{a_2}{r} < 0$.

Let $\Psi_1 = (\psi_{11}, \psi_{12}, \psi_{13})^T$ be the eigenvector of $J_1{}^T$ corresponding to the eigenvalue $\lambda_{13}{}^* = 0$. Direct calculation shows that $\Psi_1 = (0, 0, \psi_{13})^T$, where ψ_{13} is any nonzero real number. Because $\frac{\partial F}{\partial d_2} = F_{d_2} = (0, 0, -z)^T$, we obtain that $F_{d_2}\left(E_1, d_2{}^*\right) = (0, 0, 0)^T$, which yields:

$$\Psi_1{}^T\left[F_{d_2}\left(E_1, d_2{}^*\right)\right] = 0.$$

By Sotomayor's theorem, system (1) at E_1 with $d_2 = d_2{}^*$ does not experience a saddle-node bifurcation. Moreover, we have

$$\Psi_1{}^T\left[DF_{d_2}\left(E_1, d_2{}^*\right)\Phi_1\right] = -v_{13}\Psi_{13} \neq 0,$$

where DF_{d_2} represents the derivative of F_{d_2} with respect to X. Applying equation (12) at $\left(E_1, {d_2}^*\right)$ with the eigenvector Φ_1, we obtain that

$$\Psi_1{}^T\left[D^2F\left(E_1, {d_2}^*\right)(\Phi_1, \Phi_1)\right] = 2e_2a_2\beta_1{v_{13}}^2\psi_{13} \neq 0.$$

By Sotomayor's theorem, system (1) near the equilibrium point E_1 with $d_2 = {d_2}^*$ undergoes a transcritical bifurcation, but a pitchfork bifurcation cannot occur.

Theorem (9): System (1) at the specialist-free equilibrium point E_2 undergoes a transcritical bifurcation when $d_1 = e_1a_1\bar{x} + a_3\bar{z}$ $(\equiv {d_1}^*)$, but neither a saddle-node nor a pitchfork bifurcation can occur, provided

$$e_1e_3a_1a_2 + re_3a_3 \neq e_2a_2\left[kr(1-\bar{x}) + a_1\right]. \tag{14}$$

Proof. The Jacobian matrix of system (1) at the specialist-free equilibrium point E_2 with $d_1 = {d_1}^*$ takes the form:

$$J_2 = J\left(E_2, {d_1}^*\right) = \begin{bmatrix} -r\bar{x} & -kr\bar{x}(1-\bar{x}) - a_1\bar{x} & -a_2\bar{x} \\ 0 & 0 & 0 \\ e_2a_2\bar{z} & e_3a_3\bar{z} & 0 \end{bmatrix}.$$

J_2 has eigenvalues

$$\begin{aligned} {\lambda_{21}}^* &= -\frac{r\bar{x}}{2} + \frac{1}{2}\sqrt{(r\bar{x})^2 - 4e_2{a_2}^2\bar{x}\bar{z}}, \\ {\lambda_{23}}^* &= -\frac{r\bar{x}}{2} - \frac{1}{2}\sqrt{(r\bar{x})^2 - 4e_2{a_2}^2\bar{x}\bar{z}}, \end{aligned}$$

while ${\lambda_{22}}^* = 0$; hence, the necessary but not sufficient condition for a bifurcation is satisfied, and E_2 is a non-hyperbolic point.

Let $\Phi_2 = (v_{21}, v_{22}, v_{23})^T$ be the eigenvector of J_2 corresponding to the zero eigenvalue. Straightforward computation gives $\Phi_2 = (\alpha_1v_{22}, v_{22}, \alpha_2v_{22})^T$, where v_{22} represents any nonzero real number, with

$$\alpha_1 = -\frac{e_3a_3}{e_2a_2} \text{ and } \alpha_2 = \frac{re_3a_3 - \left[kr(1-\bar{x}) + a_1\right]e_2a_2}{e_2{a_2}^2}.$$

Let $\Psi_2 = (\psi_{21}, \psi_{22}, \psi_{23})^T$ be the eigenvector of $J_2{}^T$ corresponding to the zero eigenvalue. Direct calculation shows that $\Psi_2 = (0, \psi_{22}, 0)^T$, where ψ_{22} is any nonzero real number. Because $\frac{\partial F}{\partial d_1} = F_{d_1} = \left(0, -y, 0\right)^T$, we obtain that $F_{d_1}\left(E_2, {d_1}^*\right) = (0,0,0)^T$, which yields

$$\Psi_2{}^T\left[F_{d_1}\left(E_2, {d_1}^*\right)\right] = 0.$$

Thus, by Sotomayor's theorem, system (1) at E_2 with $d_1 = {d_1}^*$ does not experience a saddle-node bifurcation. Moreover, we have:

$$\Psi_2{}^T\left[DF_{d_1}\left(E_2, {d_1}^*\right)\Phi_2\right] = -v_{22}\psi_{22} \neq 0,$$

where DF_{d_1} represents the derivative of F_{d_1} with respect to X. Using equation (12) at $\left(E_2, {d_1}^*\right)$ with the eigenvector Φ_2, we obtain that

$$\Psi_2{}^T\left[D^2F\left(E_2, {d_1}^*\right)(\Phi_2, \Phi_2)\right] = (2e_1a_1\alpha_1 - 2a_3\alpha_2)\,{v_{22}}^2\psi_{22}.$$

It is easy to verify that $\Psi_2{}^T\left[D^2F\left(E_2, {d_1}^*\right)(\Phi_2, \Phi_2)\right] \neq 0$ due to condition (14). Hence, by Sotomayor's theorem, system (1) near the equilibrium point E_2 with $d_1 = {d_1}^*$ undergoes a transcritical bifurcation but a pitchfork bifurcation cannot occur.

Theorem (10): At the superpredator-free equilibrium point E_3, system (1) undergoes a transcritical bifurcation when $d_2 = e_2a_2\hat{x} + e_3a_3\hat{y}$ $(\equiv {d_2}^*)$, but neither a saddle-node nor a pitchfork bifurcation can occur, provided

$$\begin{aligned} &e_2a_2\left[kr\left(1-\hat{x}\right) + a_1(1+k\hat{y})^2\right] \neq \\ &e_3(1+k\hat{y})\left[a_3r + e_1a_1a_2(1+k\hat{y})\right]. \end{aligned} \tag{15}$$

Proof. The Jacobian matrix of system (1) at the superpredator-free equilibrium point E_3 with $d_2 = {d_2}^*$ is

$$J_3 = J\left(E_3, {d_2}^*\right) = \begin{bmatrix} -\frac{r\hat{x}}{1+k\hat{y}} & -\frac{kr\hat{x}(1-\hat{x})}{(1+k\hat{y})^2} - a_1\hat{x} & -a_2\hat{x} \\ e_1a_1\hat{y} & 0 & -a_3\hat{y} \\ 0 & 0 & 0 \end{bmatrix}.$$

J_3 has eigenvalues

$$\begin{aligned} {\lambda_{31}}^* &= -\frac{r\hat{x}}{2(1+k\hat{y})} \\ &+ \frac{1}{2}\sqrt{\left(\frac{r\hat{x}}{1+k\hat{y}}\right)^2 - 4e_1a_1\hat{y}\left(\frac{kr\hat{x}\left(1-\hat{x}\right)}{\left(1+k\hat{y}\right)^2} + a_1\hat{x}\right)}, \end{aligned}$$

$$\begin{aligned} {\lambda_{32}}^* &= -\frac{r\hat{x}}{2\left(1+k\hat{y}\right)} \\ &- \frac{1}{2}\sqrt{\left(\frac{r\hat{x}}{1+k\hat{y}}\right)^2 - 4e_1a_1\hat{y}\left(\frac{kr\hat{x}\left(1-\hat{x}\right)}{\left(1+k\hat{y}\right)^2} + a_1\hat{x}\right)}, \end{aligned}$$

while ${\lambda_{33}}^* = 0$; hence, the necessary but not sufficient condition for bifurcation is satisfied, and E_3 is a non-hyperbolic point.

Let $\Phi_3 = (v_{31}, v_{32}, v_{33})^T$ be the eigenvector of J_3 corresponding to the zero eigenvalue. Straightforward computation gives $\Phi_3 = (s_1v_{33}, s_2v_{33}, v_{33})^T$, where v_{33} represents any nonzero real number, while

$$s_1 = \frac{a_3}{e_1a_1} \text{ and } s_2 = -\left[\frac{ra_3\left(1+k\hat{y}\right) + e_1a_1a_2(1+k\hat{y})^2}{e_1a_1\left[kr\left(1-\hat{x}\right) + a_1(1+k\hat{y})^2\right]}\right].$$

Let $\Psi_3 = (\psi_{31}, \psi_{32}, \psi_{33})^T$ be the eigenvector of $J_3{}^T$ corresponding to the zero eigenvalue. Direct calculation shows that $\Psi_3 = (0, 0, \psi_{33})^T$, where ψ_{33} is any nonzero real number.

Because $\frac{\partial F}{\partial d_2} = F_{d_2} = (0,0,-z)^T$, we obtain $F_{d_2}\left(E_3, d_2{}^*\right) = (0,0,0)^T$, which yields

$$\Psi_3{}^T\left[F_{d_2}\left(E_3, d_2{}^*\right)\right] = 0.$$

Thus, by Sotomayor's theorem, system (1) at E_3 with $d_2 = d_2{}^*$ does not experience a saddle-node bifurcation. Moreover, we have:

$$\Psi_3{}^T\left[DF_{d_2}\left(E_3, d_2\right)\Phi_3\right] = -v_{33}\psi_{33} \neq 0,$$

where DF_{d_2} represents the derivative of F_{d_2} with respect to X. By using equation (12) at $\left(E_3, d_2{}^*\right)$ with the eigenvector Φ_3, we obtain that:

$$\Psi_3{}^T\left[D^2F\left(E_3, d_2{}^*\right)(\Phi_3, \Phi_3)\right] = (2e_2a_2s_1 + 2e_3a_3s_2)\, v_{33}{}^2\psi_{33}.$$

Straightforward computation shows that $\Psi_3{}^T\left[D^2F\left(E_3, d_2{}^*\right)(\Phi_3, \Phi_3)\right] \neq 0$ due to condition (15). Thus, by Sotomayor's theorem, system (1) near the equilibrium point E_3 with $d_2 = d_2{}^*$ undergoes a transcritical bifurcation, but a pitchfork bifurcation cannot occur.

Theorem (11): System (1) undergoes a saddle-node bifurcation at the coexistence equilibrium point E_4, but neither a transcritical nor a pitchfork bifurcation can occur when e_3 passes through the value $e_3{}^* = \frac{b_{12}b_{23}b_{31}}{(b_{11}b_{23}-b_{13}b_{21})a_3z^*}$, provided the following conditions hold:

$$\left(\frac{krx^*\left(1-x^*\right)}{\left(1+ky^*\right)^2} + a_1x^*\right)e_2a_2 > \left(\frac{rx^*}{1+ky^*}\right)e_3{}^*a_3, \tag{16a}$$

$$\frac{a_1a_2}{a_3}\left(\frac{e_2}{e_3{}^*} - e_1\right) - \frac{r}{\left(1+ky^*\right)} \times \left[1 - \frac{k\left(1-2x^*\right)e_2a_2}{\left(1+ky^*\right)e_3{}^*a_3} - \frac{k^2x^*\left(1-x^*\right)(e_1a_1)^2}{\left(1+ky^*\right)^2 a_3{}^2}\right] \neq 0. \tag{16b}$$

Proof. Direct computation shows that system (1) at the coexistence equilibrium point and $e_3 = e_3{}^*$ has Jacobian matrix

$$J_4 = J\left(E_4, e_3{}^*\right) = \begin{bmatrix} -\frac{rx^*}{1+ky^*} & -\frac{krx^*(1-x^*)}{(1+ky^*)^2} - a_1x^* & -a_2x^* \\ e_1a_1y^* & 0 & -a_3y^* \\ e_2a_2z^* & e_3{}^*a_3z^* & 0 \end{bmatrix} = \left[b_{ij}\right]_{3\times 3}.$$

Straightforward computation shows that $|J_4| = 0$, under condition (16a). Hence, J_4 has two eigenvalues with negative real parts, and the third one is $\lambda^* = 0$. It follows that E_4 becomes a non-hyperbolic equilibrium point.

Let $\Phi_4 = (v_{41}, v_{42}, v_{43})^T$ be the eigenvector of J_4 corresponding to the eigenvalue $\lambda^* = 0$. Straightforward computation gives $\Phi_4 = (v_{41}, \delta_1 v_{41}, \delta_2 v_{41})^T$, where v_{41} represents any nonzero real number, $\delta_1 = -\frac{b_{31}}{b_{32}{}^*} < 0$ and $\delta_2 = -\frac{b_{21}}{b_{23}} > 0$.

Let $\Psi_4 = (\psi_{41}, \psi_{42}, \psi_{43})^T$ be the eigenvector of $J_4{}^T$ corresponding to the eigenvalue $\lambda^* = 0$. Direct calculation shows that $\Psi_4 = (\psi_{41}, \mu_1\psi_{41}, \mu_2\psi_{41})^T$, where ψ_{33} is any nonzero real number, with $\mu_1 = -\frac{b_{13}}{b_{23}} < 0$ and $\mu_2 = -\frac{b_{12}}{b_{32}} > 0$.

Since $\frac{\partial F}{\partial e_3} = F_{e_3} = \left(0,0,a_3yz\right)^T$, we have $F_{e_3}\left(E_4, e_3{}^*\right) = \left(0,0,a_3y^*z^*\right)^T$, which yields

$$\Psi_4{}^T\left[F_{e_3}\left(E_4, e_3{}^*\right)\right] = a_3\mu_2y^*z^*\psi_{41} \neq 0.$$

By Sotomayor's theorem, transcritical and pitchfork bifurcations cannot occur while the first condition of the saddle-node bifurcation is satisfied. Moreover, from equation (12) with $E_4, e_3{}^*$ and Φ_4, we obtain that:

$$D^2F\left(E_4, e_3{}^*\right)(\Phi_4, \Phi_4) = 2v_{41}{}^2 \times \begin{pmatrix} -\frac{r}{1+ky^*} - \frac{kr\left(1-2x^*\right)\delta_1}{\left(1+ky^*\right)^2} - a_1\delta_1 - a_2\delta_2 + \frac{k^2rx^*\left(1-x^*\right)\delta_2{}^2}{\left(1+ky^*\right)^3} \\ e_1a_1\delta_1 - a_3\delta_1\delta_2 \\ e_2a_2\delta_2 + e_3{}^*a_3\delta_1\delta_2 \end{pmatrix}.$$

Hence,

$$\Psi_4^T\left[D^2F\left(E_4, e_3{}^*\right)(\Phi_4, \Phi_4)\right] = 2v_{41}{}^2\psi_{41} \times \left[-\frac{r}{1+ky^*} - \frac{kr\left(1-2x^*\right)\delta_1}{\left(1+ky^*\right)^2} - a_1\delta_1 - a_2\delta_2 + \frac{k^2rx^*\left(1-x^*\right)\delta_2{}^2}{\left(1+ky^*\right)^3} + e_1a_1\delta_1\mu_1 - a_3\delta_1\delta_2\mu_1 + e_2a_2\delta_2\mu_2 + e_3{}^*a_3\delta_1\delta_2\mu_2\right].$$

Further computation shows that

$$\Psi_4{}^T\left[D^2F\left(E_4, e_3{}^*\right)(\Phi_4, \Phi_4)\right] = 2v_{41}{}^2\psi_{41}\left[\frac{a_1a_2}{a_3}\left(\frac{e_2}{e_3{}^*} - e_1\right) - \frac{r}{\left(1+ky^*\right)}\left[1 - \frac{k\left(1-2x^*\right)e_2a_2}{\left(1+ky^*\right)e_3{}^*a_3} - \frac{k^2x^*\left(1-x^*\right)(e_1a_1)^2}{\left(1+ky^*\right)^2a_3{}^2}\right]\right].$$

Using condition (16b), we have $\Psi_4{}^T\left[D^2F\left(E_4, e_3{}^*\right)(\Phi_4, \Phi_4)\right] \neq 0$. Hence, system (1) has a saddle-node bifurcation at E_4 when $e_3 = e_3{}^*$.

Theorem (12): System (2) undergoes a Hopf bifurcation around E_4 when $e_3 = e_3{}^{**}$, if and only if the following conditions hold:

$$\left(\frac{krx^*\left(1-x^*\right)}{\left(1+ky^*\right)^2} + a_1x^*\right)e_2a_2 < \left(\frac{rx^*}{1+ky^*}\right)e_3a_3, \tag{17a}$$

$$\left[A(e_3{}^{**})B(e_3{}^{**})\right]' < C'(e_3{}^{**}), \tag{17b}$$

where

$$A = -b_{11} > 0,$$

$$B = -b_{12}b_{21} - b_{13}b_{31} - b_{23}b^*_{32} > 0,$$

$$C = b_{23}\left(b_{11}b^*_{32} - b_{12}b_{31}\right) - b_{13}b_{21}b^*_{32},$$

with $b^*_{32} = e_3{}^{**}a_3z^*$ and,

$$e_3{}^{**} = \frac{1}{e_1a_1a_2a_3y^*z^*}\left[\left[\frac{kr\left(1-x^*\right)}{\left(1+ky^*\right)^2} - a_1\right] \times \left(e_1a_1y^*\left(\frac{rx^*}{1+ky^*}\right) + e_2a_2a_3y^*z^*\right) + e_2a_2{}^2z^*\left(\frac{rx^*}{1+ky^*}\right)\right].$$

Proof. Consider the Jacobian matrix J_4 given in Theorem (11), where $e_3 = e_3{}^{**}$. It is simple to determine that the characteristic equation is

$$\lambda^3 + A\lambda^2 + B\lambda + C = 0. \tag{18}$$

Obviously, condition (17a) guarantees that $C > 0$. A straightforward computation shows that $AB = C$ when $e_3 = e_3{}^{**}$. Hence, the characteristic equation (18) becomes

$$\left(\lambda^2 + B\right)(\lambda + A) = 0. \tag{19}$$

Consequently, we obtain that $\lambda_1 = -A$ and $\lambda_{2,3} = \pm i\sqrt{B} = \pm i\delta_2(e_3{}^{**})$. Therefore, the Jacobian matrix has one negative real eigenvalue and two pure imaginary complex conjugates when $e_3 = e_3{}^{**}$. As a result, the first criterion for having a Hopf bifurcation is met.

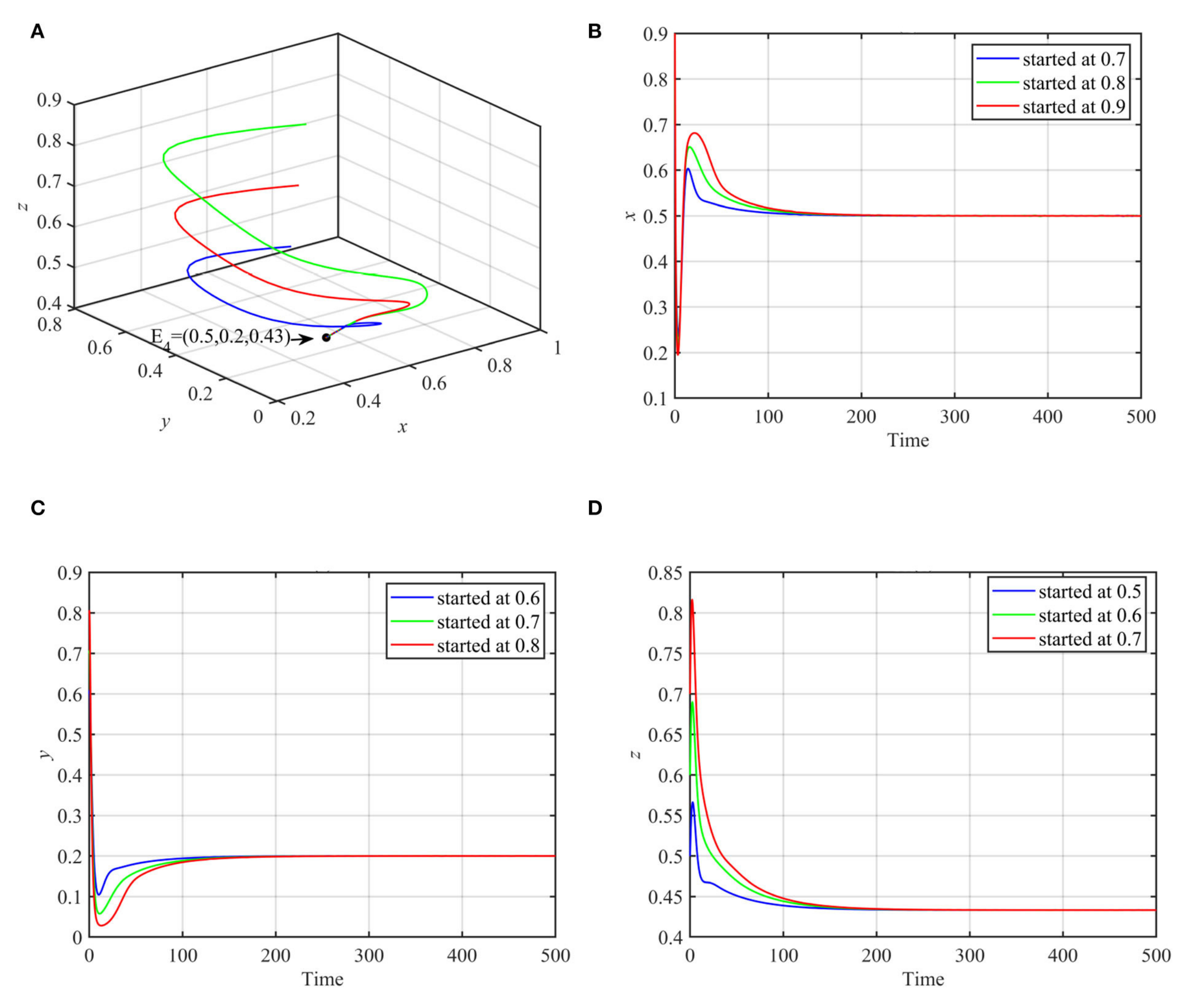

FIGURE 1
Globally asymptotically stable coexistence equilibrium point using data (17) and multiple initial conditions. **(A)** 3D-Phase portrait of the system (1). **(B)** Time series for trajectories of x. **(C)** Time series for trajectories of y. **(D)** Time series for trajectories of z.

Moreover, where e_3 belongs to the neighborhood of ${e_3}^{**}$, the eigenvalues become $\lambda_{2,3} = \delta_1(e_3) \pm i\delta_2(e_3)$.

Next, we substitute $\delta_1(e_3) + i\delta_2(e_3)$ into equation (18) and take the derivative of the resulting equation with respect to e_3. Equating their real and imaginary parts, we obtain that

$$\begin{aligned} H_1(e_3)\,\delta_1^{'}(e_3) - H_2(e_3)\,\delta_2^{'}(e_3) &= -H_3(e_3), \\ H_2(e_3)\,\delta_1^{'}(e_3) + H_1(e_3)\,\delta_2^{'}(e_3) &= -H_4(e_3), \end{aligned} \tag{20}$$

where

$$H_1(e_3) = 3\left[\delta_1(e_3)\right]^2 + 2A(e_3)\,\delta_1(e_3) - 3\left[\delta_2(e_3)\right]^2 + B(e_3).$$

$$H_2(e_3) = 6\delta_1(e_3)\,\delta_2(e_3) + 2A(e_3)\,\delta_2(e_3).$$

$$H_3(e_3) = A^{'}(e_3)\left[\delta_1(e_3)\right]^2 - A^{'}(e_3)\left[\delta_2(e_3)\right]^2 + B^{'}(e_3)\,\delta_1(e_3) + C^{'}(e_3).$$

$$H_4(e_3) = 2A^{'}(e_3)\,\delta_1(e_3)\,\delta_2(e_3) + B^{'}(e_3)\,\delta_2(e_3).$$

Solving system (20) for $\delta_1^{'}(e_3)$ gives

$$\delta_1^{'}(e_3) = -\frac{H_1(e_3)\,H_3(e_3) + H_2(e_3)\,H_4(e_3)}{\left[H_2(e_3)\right]^2 + (e_3)\left[H_2(e_3)\right]^2}.$$

The result follows if and only if $\delta_1^{'}(e_3) \neq 0$ or, equivalently, $H_1(e_3)\,H_3(e_3) + H_2(e_3)\,H_4(e_3) \neq 0$ when $e_3 = {e_3}^{**}$. Note that we have the following:

$$\delta_1\left({e_3}^{**}\right) = 0 \text{ and } \delta_2\left({e_3}^{**}\right) = \sqrt{B\left({e_3}^{**}\right)}.$$

$$H_1\left({e_3}^{**}\right) = -2B\left({e_3}^{**}\right).$$

$$H_2\left({e_3}^{**}\right) = 2A\left({e_3}^{**}\right)\sqrt{B\left({e_3}^{**}\right)}.$$

$$H_3\left({e_3}^{**}\right) = -A^{'}\left({e_3}^{**}\right)\left[B\left({e_3}^{**}\right)\right] + C^{'}\left({e_3}^{**}\right).$$

$$H_4\left({e_3}^{**}\right) = B^{'}\left({e_3}^{**}\right)\sqrt{B\left({e_3}^{**}\right)}.$$

Consequently,

$$\begin{aligned} &H_1\left({e_3}^{**}\right)H_3\left({e_3}^{**}\right) + H_2\left({e_3}^{**}\right)H_4\left({e_3}^{**}\right) \\ &\quad = 2A^{'}\left({e_3}^{**}\right)B^2\left({e_3}^{**}\right) - 2B\left({e_3}^{**}\right) \\ &\quad\quad C^{'}\left({e_3}^{**}\right) + 2A\left({e_3}^{**}\right)B^{'}\left({e_3}^{**}\right)B\left({e_3}^{**}\right) \\ &\quad = -2B\left({e_3}^{**}\right)[C^{'}\left({e_3}^{**}\right) - (A^{'}\left({e_3}^{**}\right) \\ &\quad\quad B\left({e_3}^{**}\right) + A\left({e_3}^{**}\right)B^{'}\left({e_3}^{**}\right)]. \end{aligned}$$

Condition (17b) ensures that $H_1({e_3}^{**})\,H_3({e_3}^{**}) + H_2({e_3}^{**})\,H_4({e_3}^{**}) \neq 0$.

Hence, the system has a Hopf bifurcation because $\delta_1^{'}(e_3) > 0$ under the conditions (17a)–(17b).

Numerical simulations

To illustrate the global dynamics of the system and confirm our analytical findings, we numerically simulated a

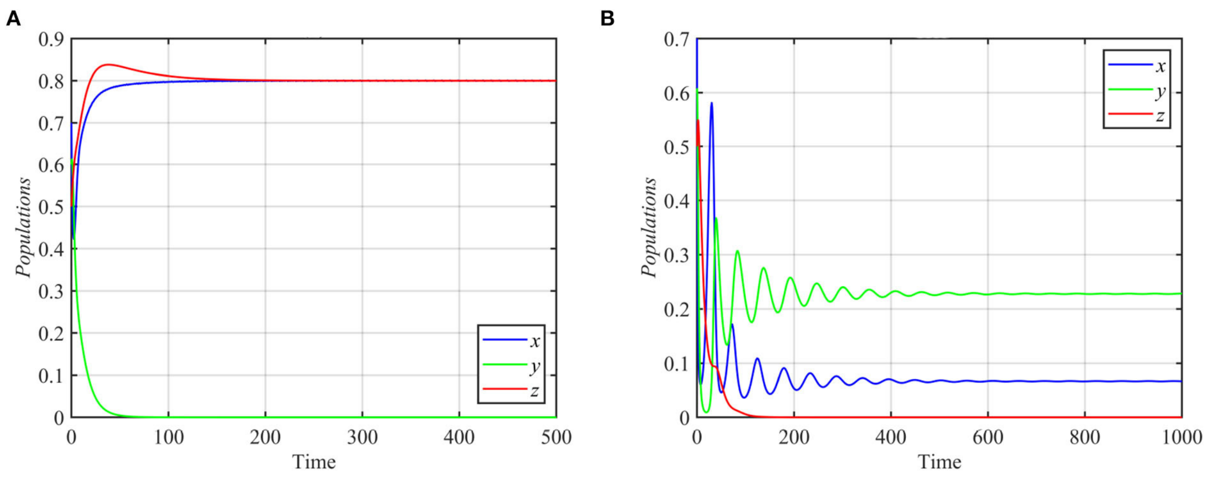

FIGURE 2
Trajectories of system (1) for different values of r, with other parameters as in equation (17). **(A)** Time series for trajectories of x, y, and z for $r = 2$, which approach $E_2 = (0.8, 0, 0.8)$. **(B)** Time series for trajectories of x, y, and z for $r = 0.3$, which approach $E_3 = (0.06, 0.22, 0)$.

hypothetical set of parameter values. Consider the following set of parameters:

$$\begin{aligned} r = 1, k = 1, a_1 = 1, a_2 = 0.5, a_3 = 0.75, e_1 = 0.75 \\ e_2 = 0.25, e_3 = 0.25, d_1 = 0.05, d_2 = 0.1. \end{aligned} \tag{21}$$

Using these data, system (1) asymptotically approaches the coexistence equilibrium point $E_4 = (0.5, 0.2, 0.43)$, as shown in Figure 1.

Next, we varied specific parameters to understand the effect of that parameter on the dynamical behavior of the system. For the values of the parameter r satisfying $r \geq 1.84$ and other parameters as in equation (17), system (1) approaches the specialist-free equilibrium point, as shown in Figure 2A for the typical value $r = 2$. For $r \leq 0.76$ and other parameters as in equation (17), system (1) asymptotically approaches the superpredator-free equilibrium point, as shown in Figure 2B.

For different values of the fear rate k with the rest of the data as given in equation (17), system (1) is solved numerically and illustrated in Figure 3.

As shown in Figure 2, the superpredator decreases as k increases, with extinction for $k > 2$. We also varied the parameter a_1 with other parameters still fixed as in equation (17). For the range $a_1 \geq 1.3$, system (1) asymptotically approaches the superpredator-free equilibrium, as shown in Figure 4A for the typical value $a_1 = 1.75$. Conversely, system (1) approaches asymptotically to the specialist-free

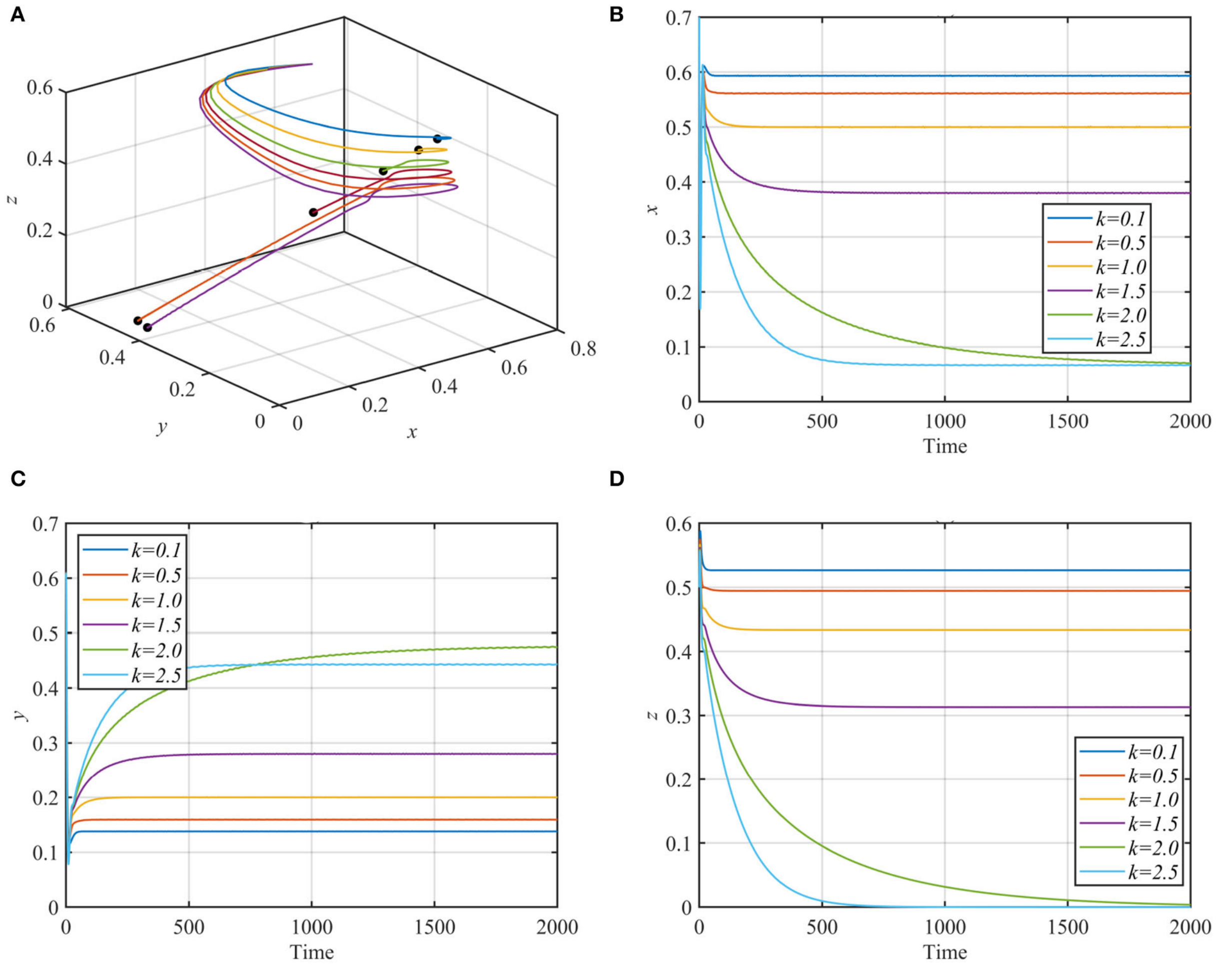

FIGURE 3
Trajectories of system (1) using data given in equation (17) with different values of k. **(A)** 3D-Phase portrait of system (1) for different values of k. **(B)** Time series for the trajectory of x, in which x decreases but remains positive as k increases. **(C)** Time series for the trajectory of y, in which y increases as k increases. **(D)** Time series for the trajectory of z, in which z decreases as k increases and approaches zero for $k > 2$.

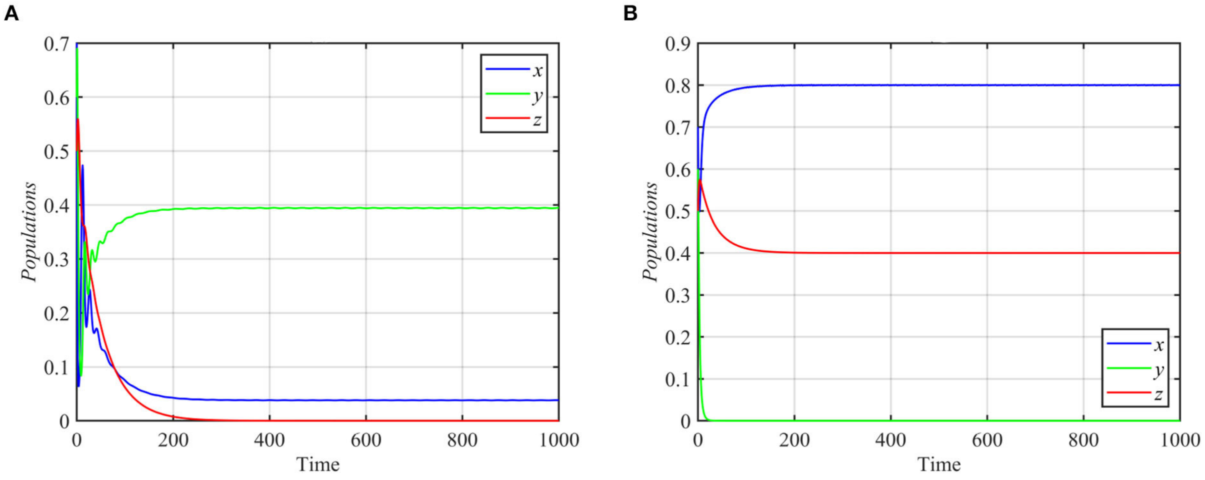

FIGURE 4

Trajectories of system (1) for different values of a_1 and other parameters as in equation (17). **(A)** Time series for trajectories of x, y, and z for $a_1 = 1.75$, which approach $E_3 = (0.03, 0.39, 0)$. **(B)** Time series for trajectories of x, y, and z for $a_1 = 0.4$, which approach $E_2 = (0.8, 0, 0.4)$.

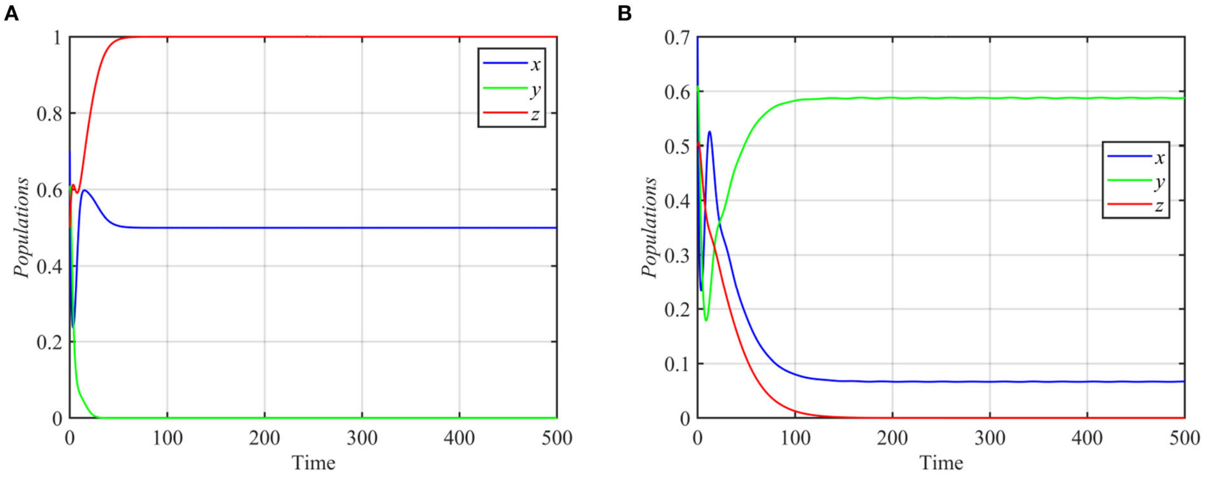

FIGURE 5

Trajectories of system (1) for different values of e_2 and e_3, with other parameters as in equation (17). **(A)** Time series for trajectories of x, y, and z for $e_2 = 0.4$, which approach $E_2 = (0.5, 0, 1)$. **(B)** Time series for trajectories of x, y, and z for $e_3 = 0.1$, which approach $E_3 = (0.06, 0.58, 0)$.

equilibrium point, as shown in Figure 4B for the typical value $a_1 = 0.4$.

System (1) still asymptotically approaches the coexistence equilibrium point for the data given in equation (17), when e_1 or e_3 increases or when e_2 decreases. However, for $e_1 \leq 0.44$, system (1) asymptotically approaches the specialist-free equilibrium point $E_2 = (0.8, 0, 0.4)$, as shown in Figure 4B. For $e_2 \geq 0.3$ or $e_3 \leq 0.2$ and the other parameters as in equation (17), the trajectories of system (1) asymptotically approach the specialist-free equilibrium point or the superpredator-free equilibrium point as shown in Figure 5.

Further investigation for the effect of varying parameters a_2 and a_3 while keeping the rest of the parameters as in equation (17) shows that the parameter a_2 has similar effects as the parameter e_2 with a bifurcation point at $a_2 = 0.63$. However, parameter a_3 has similar effects as parameter r, with two bifurcation points: $a_3 = 1.38$ and $a_3 = 0.62$.

Finally, for $d_1 \geq 0.31$ and the rest of the parameters as in equation (17), the trajectories of system (1) asymptotically approach the specialist-free equilibrium point, as shown in Figure 6A for the typical value $d_1 = 0.4$. However, system (1) approaches the coexistence equilibrium point otherwise. On the

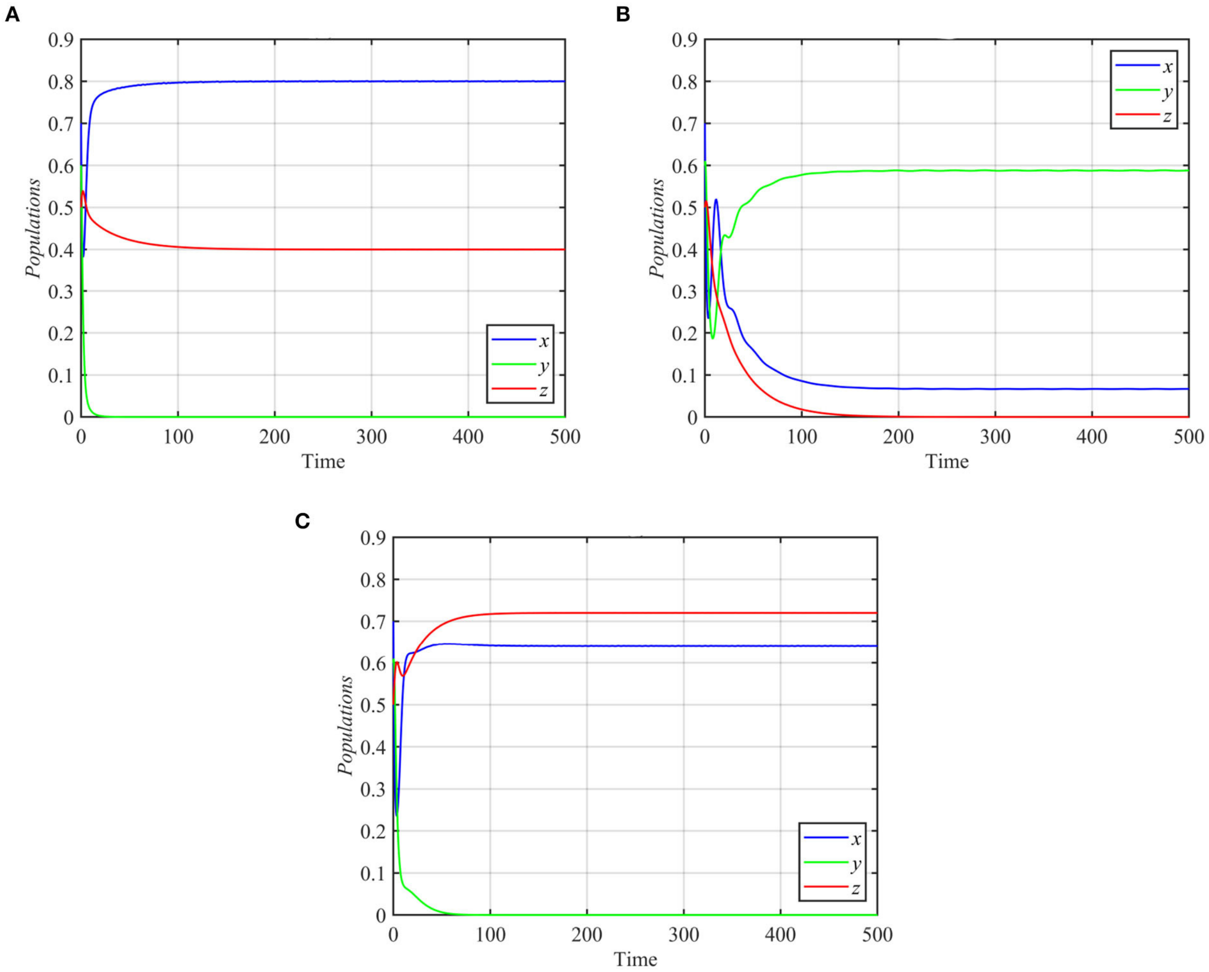

FIGURE 6
Trajectories of system (1) for different values of d_1 and d_2, with other parameters as in equation (17). **(A)** Time series for trajectories of x, y, and z for $d_1 = 0.4$, which approach $E_2 = (0.8, 0, 0.4)$. **(B)** Time series for trajectories of x, y, and z for $d_2 = 0.15$, which approach $E_3 = (0.06, 0.58, 0)$. **(C)** Time series for trajectories of x, y, and z for $d_2 = 0.08$, which approach $E_2 = (0.64, 0, 0.72)$.

other hand, for $d_2 \geq 0.12$ or $d_2 \leq 0.08$ and the other parameters as in equation (17), trajectories of system (1) asymptotically approach either the superpredator-free equilibrium point or the specialist-free equilibrium point, as shown in Figures 6B,C for the typical values $d_2 = 0.15$ and $d_2 = 0.08$, respectively.

Varying parameters d_1 and d_2 together so that they satisfy conditions (7a) and (7b) while keeping other parameters as in equation (17) makes the trajectories of system (1) asymptotically approach the axial equilibrium point $E_1 = (1, 0, 0)$ as shown in Figure 7.

Discussion

Classical intraguild predation food web models have been extensively studied, but relatively little work has been done on the effect of fear on the prey. To the best of our knowledge, this is the first model considering prey fear of only the specialist predator. We determined the equilibria and global stability properties of the model, found bifurcations, and illustrated the theoretical behavior with numerical simulations.

Many previous studies have found that three-species intraguild predation models, in which a superpredator (IG predator) both attacks and competes with a specialist predator (IG prey), are often unstable, either because one consumer is excluded or because long feedback loops produce sustained oscillations [30]. Despite this, many natural IGP systems continue to thrive. Many empirical intraguild predation systems are entrenched in communities with alternative prey species, and standard models of intraguild predation simplify actual systems in significant ways that could affect persistence. Holt and Huxel [30] presented results of theoretical explorations of how alternative prey can influence the persistence and stability of a focal intraguild predation interaction. They reviewed the

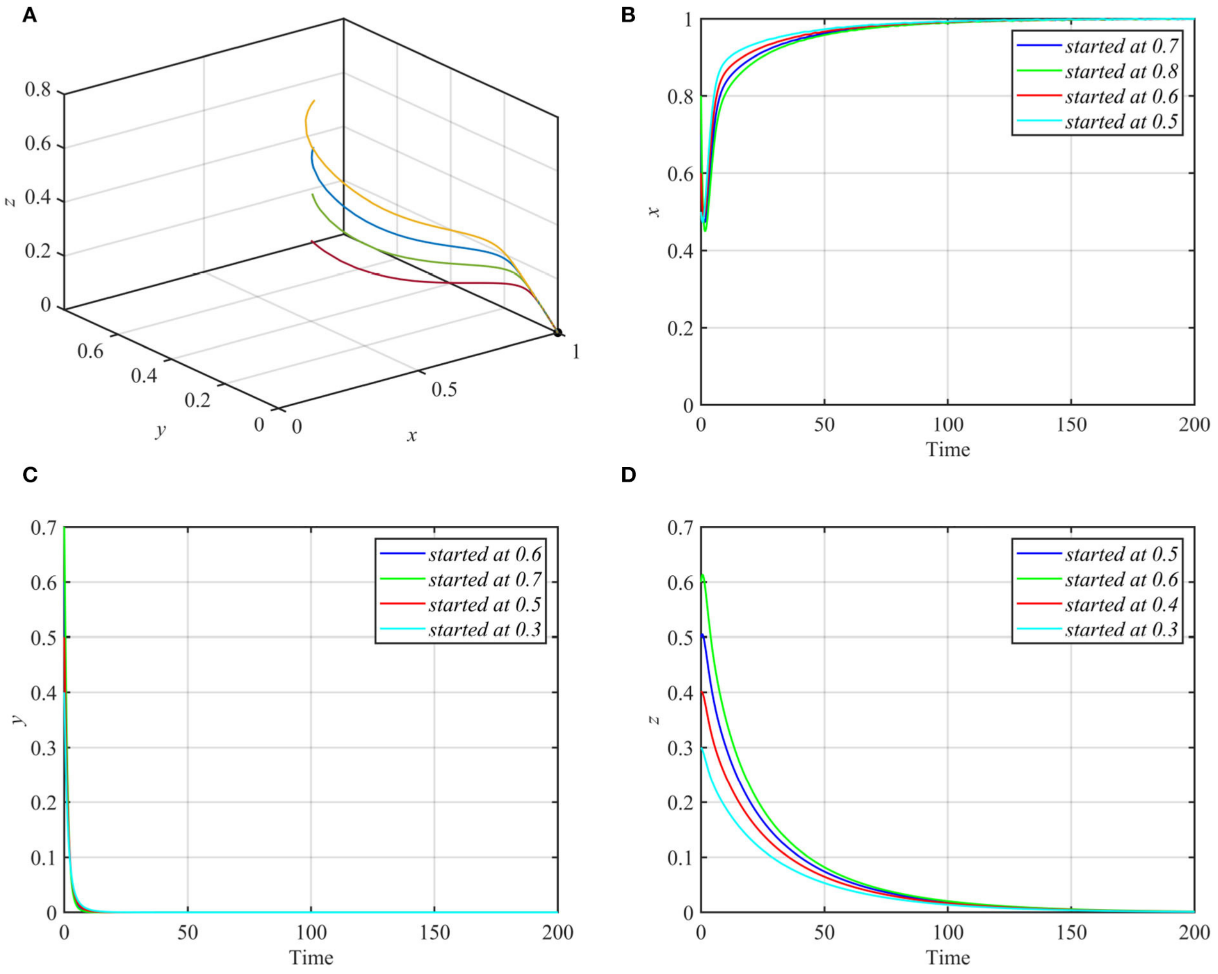

FIGURE 7
Globally asymptotically stable axial equilibrium point for $d_1 = 0.8$, $d_2 = 0.15$ and other parameters as in equation (17). **(A)** 3D-Phase portrait. **(B)** Time series for trajectories of x. **(C)** Time series for trajectories of y. **(D)** Time series for trajectories of z.

key conclusions of standard three-species IGP theory and then presented results of theoretical explorations of how alternative prey can influence the persistence and stability of a focal intraguild predation interaction. Conversely, Bai et al. [10] indicated that the intraguild predation food web model has rich and complicated dynamic behavior, and a large Allee effect in the basal prey raises the extinction risk of not only the basal prey but also the IG prey or/and IG predator.

Hossain et al. investigated fear in an intraguild predation model, in which the growth rate of a specialist predator (IG prey) is reduced due to the cost of fear of a superpredator (IG predator), and the growth rate of a basal prey is suppressed due to the cost of fear of both the IG prey and the IG predator [20]. In a three-species food chain system, they found that omnivory can cause chaos in the absence of fear. Fear, on the other hand, can help to keep the chaos under control. They also discovered that the system exhibits bistability between the IG prey-free and IG predator-free equilibrium, as well as bistability between IG prey-free and interior equilibria. Furthermore, they showed that the system can display numerous stable limit cycles for a given set of parameter values.

However, in our study, instilling the fear of a specialist predator (IG prey) in the presence of a superpredator (IG predator) had the unintended consequence of eradicating the superpredator. This demonstrates the often-surprising complexity of food-chain dynamics and has not been observed in previous articles dedicated to the study of fear [23–27]. In contrast, if the prey's intrinsic growth rate is sufficiently high, the IG prey can be eradicated, while the IG predator can be removed if the prey's intrinsic growth rate is sufficiently low. Coexistence or the eradication of both predators are other possibilities. As a result, system (1) has rich dynamical behavior, is sensitive to parameter changes, and at least one bifurcation point exists for each of the parameters. This result is comparable to decreasing the productivity of a resource (comparable to a higher fear effect in the prey in this manuscript) resulting in a reduction in the density of the highest trophic level [31].

The most important parameters that influenced the outcome were, in order, the growth rate r, the fear effect k, predation upon the prey by the specialist predator a_1, the conversion factor between the prey and the superpredator e_2, the conversion factor between the specialist predator and the superpredator e_3, the death rate of the specialist predator d_1, and the natural death rate of the superpredator d_2.

Our model contains several limitations, which should be acknowledged. We only looked at the prey's fear of the specialized predator, not of the superpredator, and we ignored the specialist predator's fear of the superpredator. Our interpretation of such a case is that the pressure of the superpredator on the basal prey is much lower than that of a specialist predator due to the existence of alternative food sources. Mass-action kinetics and a conversion factor are used to model each predator's attack rates, which is a simplification of the genuine dynamics. Finally, the predators were completely reliant on a single food source, which is not always the case.

As a result, the dynamics of a food web in which the prey is afraid of one predator but not the other can produce unexpected results. In the absence of other fear effects, future research will consider the prey's fear of the superpredator but not the specialized predator; the specialist predator's fear of the superpredator could also be incorporated.

Data availability statement

The original contributions presented in the study are included in the article/supplementary files, further inquiries can be directed to the corresponding author.

Author contributions

NF developed the model, wrote the initial draft, conducted analysis, and performed numerical simulations. RN conducted analysis and performed numerical simulations. MH designed the study. SS? rewrote and edited and manuscript. All authors contributed to the article and approved the submitted version.

Funding

SS? is supported by an NSERC Discovery Grant. For citation purposes, please note that the question mark is part of her name.

Conflict of interest

The authors declare that the research was conducted in the absence of any commercial or financial relationships that could be construed as a potential conflict of interest.

Publisher's note

References

1. Thompson RM, Brose U, Dunne JA, Hall RO, Hladyz S, Kitching RL, et al. Food webs: reconciling the structure and function of biodiversity. *Trends Ecol Evolut.* (2012) 27:689–697. doi: 10.1016/j.tree.2012.08.005

2. Allesina S, Tang S. Stability criteria for complex ecosystems. *Nature.* (2012) 483:205–08. doi: 10.1038/nature10832

3. Aziz-Alaoui MA. Study of a leslie gower type tri-trophic population model. *Chaos Solitons Fractals.* (2002) 14:1275–1293. doi: 10.1016/S0960-0779(02)00079-6

4. Gakkhar S, Singh B, Naji RK. Dynamical behavior of two predators competing over a single prey. *BioSystem.* (2007) 90:808–817. doi: 10.1016/j.biosystems.2007.04.003

5. Gakkhar S, Naji RK. On a food web consisting of a specialist and generalist predator. *J Biol Syst.* (2003) 11:365–376. doi: 10.1142/S02183390030 00956

6. Gakkhar S, Naji RK. Order and chaos in a food web consisting of a predator and two independent preys. *Commun Nonlinear Sci Numer Simulat.* (2005) 10:105–120. doi: 10.1016/S1007-5704(03)00120-5

7. Klebanoff A, Hastings A. Chaos in one predator two prey model: general results from bifurcation theory. *Math. Biosciences.* (1994) 122:221–223. doi: 10.1016/0025-5564(94)90059-0

8. Holt RD, Polis GA. A theoretical framework for intraguild predation. *Am Natur.* (1997) 149:745–764. doi: 10.1086/286018

9. Tanabe K, Namba T. Omnivory creates chaos in simple food web models. *Ecology.* (2005) 86:3411–3414. doi: 10.1890/05-0720

10. Bai YK, Ruan S, Wang L. Dynamics of an intraguild predation food web model with strong Allee effect in the basal prey. *Nonlinear Anal Real World Appl.* (2021) 58:103206. doi: 10.1016/j.nonrwa.2020.103206

11. Sabelis MW. Predatory arthropods. In: *Natural enemies, the population biology of predators, parasites and diseases*, eds M. J. Crawley (Oxford: Blackwell Scientific) (1992). p. 225–264. doi: 10.1002/9781444314076.ch10

12. Crowder DW, Snyder WE. Eating their way to the top? Mechanisms underlying the 456 success of invasive generalist predators. *Biol Invas.* (2010) 12:2857–2876. doi: 10.1007/s10530-010-9733-8

13. Schreiber SJ. Generalist and specialist predators that mediate permanence in ecological communities. *J. Math. Biol.* (1997) 36:133–148 doi: 10.1007/s002850050094

14. Lima S, Dill LM. Behavioral decisions made under the risk of predation: a review and prospectus. *Can. J. Zool.* (1990) 68:619–640. doi: 10.1139/z90-092

15. Panday P, Pal N, Samanta S, Chattopadhyay J. Stability and bifurcation analysis of a three-species food chain model with fear. *Int J Bifurcation Chaos.* (2018) 28:1850009. doi: 10.1142/S0218127418500098

16. Clinchy LMDi, Roberts D, Zanette LY. Fear of large carnivores causes a trophic cascade. *Nat Commun.* (2016) 7:10698. doi: 10.1038/ncomms10698

17. Panday NP, Samanta S, Chattopadhyay J. A three species food chain model with fear induced trophic cascade. *Int J Appl Comput Math.* (2019) 5:1–26. doi: 10.1007/s40819-019-0688-x

18. Panday P, Samanta S, Pal N, Chattopadhyay J. Delay induced multiple stability switch and chaos in a predator–prey model with fear effect. *Math Comput Simulat*. (2020) 172:134–58. doi: 10.1016/j.matcom.2019.12.015

19. Cong MF, Zou X. Dynamics of a three-species food chain model with fear effect. *Commun Nonlinear Sci Numer Simulat.* (2021) 99:105809. doi: 10.1016/j.cnsns.2021.105809

20. Hossain NP, Samanta S, Chattopadhyay J. Fear induced stabilization in an intraguild predation model international. *J Bifurcation Chaos.* (2020) 30:2050053. doi: 10.1142/S0218127420500534

21. Mukherjee D. Role of fear in predator–prey system with intraspecific competition. *Math Comput Simulat.* (2020) 177: 263–275. doi: 10.1016/j.matcom.2020.04.025

22. Ibrahim HA, Naji RK. Chaos in beddington–deangelis food chain model with fear. *J Phys Conf Ser*. (2020) 1591:012082. doi: 10.1088/1742-6596/1591/1/012082

23. Mondal B, Roy S, Ghosh U, Tiwari PK. A systematic study of autonomous and nonautonomous predator–prey models for the combined effects of fear, refuge, cooperation and harvesting. *Eur Phys J Plus.* (2022) 137:724. doi: 10.1140/epjp/s13360-022-02915-0

24. Roy S, Tiwari PK, Nayak H, Martcheva M. Effects of fear, refuge and hunting cooperation in a seasonally forced eco-epidemic model with selective predation. *Eur Phys J Plus.* (2022) 137:1–31. doi: 10.1140/epjp/s13360-022-02751-2

25. Maity PKTi, Pal S. An ecoepidemic seasonally forced model for the combined effects of fear, additional foods and selective predation. *J Biol Syst.* (2022) 12:1–37. doi: 10.1142/S0218339022500103

26. Pal PKTi, Pal N. Bifurcations, chaos, and multistability in a nonautonomous predator–prey model with fear Chaos: an interdisciplinary. *J Nonlinear Sci.* (2021) 31:123–34. doi: 10.1063/5.0067046

27. Tiwari PK, Verma M, Pal S, Kang Y, Misra AK. A delay nonautonomous predator–prey model for the effects of fear, refuge and hunting cooperation. *J Biol Syst.* (2021) 29:927–69. doi: 10.1142/S0218339021500236

28. Wang X, Zanette L, Zou X. Modelling the fear effect in predator–prey interactions. *J Math Biol.* (2016) 73:1179–1204. doi: 10.1007/s00285-016-0989-1

29. Perko L. *Differential Equations and Dynamical Systems, Volume 7*. New York: Springer (1996). doi: 10.1007/978-1-4684-0249-0

30. Holt RD, Huxel GR. Alternative prey and the dynamics of intraguild predation: theoretical perspectives. *Ecology*. (2007) 88:2706–2712. doi: 10.1890/06-1525.1

31. Gurney W, Nisbet RM. *Ecological Dynamics*. Oxford: Oxford University Press. (1998).